Glucose-dependent docking and SNARE protein-mediated exocytosis in mouse pancreatic alpha-cell.

Andersson, Sofia; Pedersen, Morten Gram; Vikman, Jenny; Eliasson, Lena

Published in:
Pflügers Archiv

DOI:
10.1007/s00424-011-0979-5

2011

Glucose-dependent docking and SNARE-protein mediated exocytosis in mouse pancreatic alpha-cell

Sofia A Andersson[1], Morten G Pedersen[1], Jenny Vikman[1,2] and Lena Eliasson[1]*

[1]Islet Cell Exocytosis, Department of Clinical Sciences Malmö Lund University Diabetes Centre, Lund University, Malmö, Sweden. [2]Current address: Department of Sport Sciences, Malmö University, Malmö, Sweden

*Address for correspondence: Lena Eliasson, Islet Cell Exocytosis, Lund University Diabetes Centre, CRC 91-11, SUS Malmö entrance 72, 205 02 Malmö, Sweden, phone:+46 40 391153, fax +46 40 391222, email: lena.eliasson@med.lu.se

Running title: *SNAP25 and syntaxin1A in alpha cell exocytosis*

Keywords: islet, alpha-cell, exocytosis, glucose-dependence, Syntaxin 1A, SNAP-25, TEM, capacitance measurements

Abstract

The function of alpha-cells in patients with type 2 diabetes (T2D) is often disturbed; glucagon secretion is increased at hyperglycaemia, yet fails to respond to hypoglycaemia. A crucial mechanism behind the fine-tuned release of glucagon relies in the exocytotic machinery including SNARE proteins. Here we aimed to investigate the temporal role of syntaxin 1A and SNAP-25 in mouse alpha-cell exocytosis. First, we used confocal imaging to investigate glucose-dependency in the localisation of SNAP-25 and syntaxin 1A. SNAP-25 was mainly distributed in the plasma membrane at 2.8 mM glucose whereas the syntaxin 1A distribution in the plasma membrane, as compared to the cytosolic fraction, was highest at 8.3 mM glucose. Further, following inclusion of an antibody against SNAP-25 or syntaxin 1A, exocytosis evoked by a train of ten depolarisations and measured as an increase in membrane capacitance was reduced by ~50%. Closer inspection revealed a reduction in the refilling of granules from the reserve pool (RP), but also showed a decreased size of the readily releasable pool (RRP) by ~45%. Disparate from the situation in pancreatic beta-cells, the voltage-dependent Ca^{2+}-current was not reduced, but the Ca^{2+}-sensitivity of exocytosis decreased by the antibody against syntaxin 1A. Finally, ultrastructural analysis revealed that the number of docked granules was >2-fold higher at 16.7 mM than at 1 mM glucose. We conclude that syntaxin 1A and SNAP-25 are necessary for alpha-cell exocytosis and regulate fusion of granules belonging to both the RRP and RP without affecting the Ca^{2+}-current.

Introduction

The blood glucose level is mainly controlled by the pancreatic hormones insulin and glucagon, released from the beta - and alpha-cells, respectively. Intriguingly enough, they are activated by opposing levels of glucose where insulin counteract high blood glucose by initiating glucose uptake in muscle and fat tissue, and glucagon increases blood glucose levels by stimulating release of glucose from the glycogen storage in the liver [5]. Escalating glucose concentrations results in a concentration-dependent acceleration of glucose metabolism in both alpha- and beta-cells [8]. Yet glucagon secretion is inhibited at glucose concentrations at which insulin secretion is stimulated. In the beta-cell, glucose metabolism is followed by a closure of ATP-dependent K^+-channels (K_{ATP}-channels) whereby positively charged potassium ions retained within the cell will increase the cell membrane potential enough to activate downstream voltage-dependent Ca^{2+}-channels [29]. The direct triggering pathway of glucose differs in the mouse alpha-cells in that they contain voltage-dependent Na^+-channels downstream from the K_{ATP}-channels [30]. The increased membrane potential caused by the closure of K_{ATP}-channels following high glucose metabolism will inactivate the Na^+-channels and inhibit glucagon secretion [22]. Instead, low glucose levels render the K_{ATP}-channels partly open shifting the membrane potential enough to activate the Na^+-channels and downstream Ca^{2+}-channels [13,22]. The concomitant influx of Ca^{2+} is essential for release of glucagon via Ca^{2+}-dependent exocytosis [2,14].

Ca^{2+}-dependent exocytosis in electrically excitable cells, involves the formation of a SNARE-complex [9,16] consisting of the t-SNARE proteins syntaxin 1A and SNAP-25, and the v-SNARE protein VAMP2 (vesicle associated membrane protein 2). SNAP-25 is attached to the plasma membrane through palmitoylation of four cystein-rich residues in the central part of the protein, whereas syntaxin 1A and VAMP2 are integrated by a carboxyterminal transmembrane domain in the plasma and granular membrane, respectively. The creation of the SNARE-complex brings the granular membrane in close contact with the plasma membrane which enables fusion to take place [11]. Transport of syntaxin 1A to the plasma membrane has been proposed to require Munc-18 and syntaxin 1A has in turn been suggested to be required for the transport of SNAP-25 [32].

Glucagon is contained in ~250 nm large dense core granules [2,12] and we have earlier suggested that these granules reside in different functional pools prior to release [2]. The majority of the granules are situated within a large reserve pool (RP) that needs to be mobilised to the release-site prior to fusion. A smaller fraction of the granules are suggested to be primed and belong to a readily releasable pool of granules (RRP) situated at the release site, in similarity to the situation in pancreatic beta-cells [1] and other neuroendocrine cells [23]. Refilling of granules from RP is facilitated by glucose [26] and by cAMP-dependent activation of PKA [14]. Exocytosis of primed granules in the RRP of the alpha-cell is controlled by influx of Ca^{2+} through N-type Ca^{2+}-channels in the absence of cAMP, and through L-type Ca^{2+}-channels in the presence of high levels of cAMP [6,14]. In mouse beta-cells, rapid exocytosis is under the control of L-type Ca^{2+}-channels whereas refilling of granules is controlled by influx through R-type Ca^{2+}- channels [19]. Other than directly affecting exocytosis, SNAP-25 and syntaxin 1A have also been suggested to modulate the voltage-dependent Ca^{2+} channels [9,16], however with conflicting results. For example studies in pancreatic mouse beta-cells using antibodies against syntaxin 1 suggests that syntaxin 1 stimulates the Ca^{2+}-influx through voltage-gated Ca^{2+}-

channels [40,36], whereas experiments using a mouse over-expressing syntaxin 1A hypothesize the opposite [20].

SNAP-25 and syntaxin 1A have been demonstrated to be present in glucagon secreting cells [38] but to our knowledge no study has earlier addressed the temporal aspects of these proteins in relation to the different functional pools. Here we have used confocal microscopy to investigate glucose-dependent localization of SNAP-25 and syntaxin 1A. In addition, we investigated the exocytotic process by high-resolution capacitance measurements in combination with the patch-clamp technique on single alpha-cells in which antibodies against syntaxin 1A or SNAP-25 where induced through the patch-pipette. Finally, we have used transmission electron microscopy (TEM) to investigate the glucose dependence of granule docking.

Methods

Cells and cell culture.

In all experiments islets or single alpha-cells from NMRI mice were used. The experimental procedure has been approved by the Lund-Malmö ethical committee. Islets were isolated from pancreas using collagenase digestion as previously described [2]. The islets were then carefully picked in albumin coated Petri dishes (1mg albumin/ml Hanks) on ice to remove debris. For single cell experiments, islets were dissociated in Ca^{2+}-free buffer and the dispersed cell suspension was plated in 35-mm plastic Petri dishes (electrophysiology) or glass coverslips (immunohistochemistry). The cells were maintained in tissue culture for up to 2 days in RPMI 1640 medium containing 10 mM glucose, 5 % Foetal Calf Serum, 100 IU/ml penicillin and 10µg/ml streptomycin.

Immunohistochemistry and confocal microscopy

After culture overnight cells were preincubated for 30 minutes at 37^{o}C in KRB solution (pH 7.4) containing (in mM) 120 NaCl, 25$NaHCO_3$, 4.7 KCl, 1.2 $MgSO_4$, 2.5 $CaCl_2$, 1.2 KH_2PO, 10 HEPES and 1 mg/ml albumin and supplemented with 2.8 mM glucose. The solution was gassed with 95% O_2 and 5% CO_2 to obtain constant pH and oxygenation. Thereafter, cells were incubated for 60 minutes in KRB containing 2.8 mM, 8.3 mM or 16.7 mM glucose as indicated. Following incubation, cells were fixated with 150 µl 3% paraformaldehyde (PFA) in K-pipes with pH 6.8 (Sigma, Stockholm, Sweden) for 5 min at room temperature (RT) before a second fixation with 150 µl 3% PFA in NaB4O7 with pH 11 incubated 5 min at RT. Following washing with 200 µl PBS x2, the cells were permeabilised in 100 µl 0.1% Triton X-100 in PBS for 30 min. Thereafter, the cells were washed x1 in PBS and incubated 15 min with 100 µl 5% Normal Donkey Serum (NDS) to avoid non-specific binding. Primary antibodies against Mouse-SNAP-25 (SYSY 111 011), Rabbit-Syntaxin1A (StressGene 910 424) and Guinea Pig-Glucagon (B-GP 310-1) were added over night (1:100, 1:100 and 1:250 in 5% NDS-PBS respectively) and refrigerated. Following day, the cells were washed x2 with 200 µl PBS, then incubated 10 min with 100 µl 5% NDS-PBS at RT, before incubated 1 hour in the dark with 100 µl secondary antibody in 5% NDS-PBS (Donkey- Cy-5 (Jackson 715-175-151) 1:200; Donkey- DyeLight488 (Jackson 711-485-152) 1:100 and Donkey-Cy-3 (Jackson 706-165-148) 1:200 respectively). Next, the cells were washed with 200 µl PBS x 3 and post fixated with 200 µl 3% PFA for 10 min at RT. Following washing x3 with 200 µl PBS, a final wash x1 with 200 µl sterile-filtered mp-H_2O were performed. After proper time to dry, the cells were mounted onto object glass using mounting medium before confocal microscopy analysis.

Excitation of Cy-5, DyeLight488 and Cy-3 was performed on a Zeiss LSM510 confocal microscope (Carl Zeiss, Jena, Germany) using the 633 nm, 488 nm and 543 nm lines respectively. Emitted light passed through the BP650-710 filter (Cy-5), BP500-530 (DyeLight488) and BP650-615 (Cy3) filter and was visualized using the 63x/1.3NA oil objective. Scanning of the samples was performed sequentially with the appropriate settings for each label to minimize crosstalk, and evaluation was done using the Zeiss LSM Image examiner.

Unspecific binding of the secondary antibodies was excluded by control experiments performed in the absence of primary antibodies. Localization of SNAP-25 and syntaxin 1A was calculated from the measurements of mean fluorescence intensity I1 in an area A1 within 0.5 µm from the plasma membrane and the mean fluorescence intensity I2 in an area A2 corresponding to the intracellular region in the absence of the area occupied by the nucleus. Measurements of mean fluorescence intensity and calculation of co-localisation was performed using the ZEN 2008 software (Carl Zeiss, Jena, Germany).

Electrophysiology

Patch pipettes were pulled from borosilicate glass capillaries, coated with Sylgard (Dow Corning, Midland, MI, USA) and fire-polished. The pipette resistance was 3-6 MΩ when the pipettes were filled with the intracellular solutions specified below. Experiments were conducted on single alpha-cells within a Petri dish containing dispersed islet cells. Alpha-cells were distinguished from pancreatic beta-cells by the difference in Na^+-channel inactivation [13] and cell size <6.1 pF [2]. Experiments were performed using the standard whole-cell configuration, allowing intracellular application of the antibodies. To allow complete influx of the antibodies, the first depolarization was applied ≥ 2 min after establishment of the whole-cell configuration [4].

Capacitance measurements were used to measure exocytosis. This is possible since the increase in membrane capacitance is proportional to the increase in membrane area caused by the fusion of granules with the plasma membrane. Exocytosis was elicited by trains of ten 500-ms voltage-clamp depolarisations ranging from -70 to 0 mV applied at 1 Hz, or by single depolarisations of variable pulse duration (5-850 ms), and the whole-cell currents were recorded using an EPC-9 patch-clamp amplifier and the software Pulse (Heka Elektronik, Lamprecht/Pfalz, Germany; ver 8-31). Changes in cell capacitance were measured using the software-based lock-in application that adds sine waves with a frequency of 500-1000 Hz to the holding potential of the amplifier.

The standard extracellular solution consisted of (in mM) 118 NaCl, 20 tetraethyl-ammonium chloride (TEA-Cl; to block voltage-gated K^+-currents), 5.6 KCl, 2.6 $CaCl_2$, 1.2 $MgCl_2$, 5 glucose and 5 Hepes (pH 7.4 using NaOH). The pipette solutions contained 125 Cs-Glut, 10 NaCl, 10 CsCl, 1 $MgCl_2$, 0.05 EGTA, 3 Mg-ATP, 10 Hepes (pH 7.15 using CsOH) and 0.1 cAMP. Where indicated, the pipette solution was supplemented with either a rabbit polyclonal anti-syntaxin 1A (diluted 1:100; StressGen, Biothechnologies Corp.), rabbit anti-SNAP-25 (diluted 1:200; StressGen, Biotechnologies Corp.) or rabbit IgG (Santa Cruz Biotechnology, Santa Cruz, CA, USA).

Transmission electron microscopy

Freshly isolated islets were pre-incubated on rotating water bath at 37^{o}C for 30 minutes in KRB supplemented with 2.8 mM glucose. The samples were gassed with 95% O_2 and 5% CO_2 to obtain constant pH and oxygenation. After removal of the pre-incubation solution, islets were incubated in KRB containing 1 mM, 8.3 mM or 16.7 mM glucose for 1h. Following stimulation, the solution was removed and the islets were fixated in 2.5 % Glutaraldehyde (GA) in freshly

prepared Millionig buffer and refrigerated for 2h. Following wash in Millionig-buffer, the islets were post-fixated in osmium tetroxide (1%) for 1h, and then washed carefully with Millionig solution. Thereafter, the islets were dehydrated and embedded in AGAR 100 (Oxford Instruments Nordiska AB, Sweden) before being cut into 70-90 nm ultrathin sections with preferential on the peripheral sections of the islets to get access to maximum amount of alpha-cells. The sections were put on Cu-grids and contrasted with uranyl acetate and lead citrate before examined in a JEM 1230 electron microscope (JEOL-USA. Inc., MA, USA). Micrographs were analysed with respect to the intracellular granular distribution using similar methods that have been described elsewhere [35]. The apparent diameter of individual granules was determined with the image processing software Scion Image (NIH freeware) and the exact diameter was calculated as described elsewhere [24]. The granule volume density (Nv) and surface density (Ns) were calculated using in-house software programmed in MatLab (Matlab14).

Data Analysis

Data are represented as means ± SEM. Differences between groups were tested using Students t-test and multiple comparisons were corrected using the Holm-Bonferroni method.

For the analysis of calcium sensitivity of exocytosis, Ca^{2+}-currents were inspected carefully, and data with large leak currents or high amounts of noise were discarded from the analysis. In a statistical pre-analysis, we fitted linear models for regression of changes in membrane capacitance (ΔC_m) on the Ca^{2+} charge (Q_{Ca}), taking the differences between cells into account. Because a significant between-cell variation was present within both the control and anti-syntaxin 1A groups (F-tests, $p<1e^{-15}$), a second more appropriate analysis was performed by fitting a linear mixed-effects model [27], with treatment group as fixed effect and cell as random effect, to the data. Since capacitance is negligible in the absence of calcium entry, the linear fits were constrained to $(Q_{Ca},\Delta C_m)=(0,0)$. The statistical software R was used, in particular the lme function of the nlme R-package [27]. Parameter estimates are given with standard errors and p-values from two-sided Student t-tests.

Results

Glucose-dependent localisation of SNAP-25 and syntaxin 1A in mouse alpha-cells

First, we investigated the glucose dependent distribution of SNAP-25 and syntaxin 1A using confocal microscopy (Fig 1a). The identity of the alpha-cells was established by immunoreactivity for glucagon. SNAP-25 and syntaxin 1A localisation was evaluated following incubation in 2.8 mM, 8.3 mM or 16.7 mM glucose prior to fixation. SNAP-25 was mainly present in the plasma membrane at the low glucose concentration, with increasing presence in the cytosolic region parallel to higher glucose concentrations (Fig 1a). Syntaxin 1A fluorescence was present in both the intracellular and plasma membrane regions under all three conditions. The distribution was quantified by calculating the ratio (R) of the fluorescence intensity in the vicinity of the plasma membrane (in a region 0.5 µm from the plasma membrane; I1) to that in the intracellular region (in the absence of the nuclear region; I2) as illustrated in Fig. 1b. The quantification (Fig. 1c) verified that the ratio of SNAP-25 fluorescence intensity at the plasma membrane versus the cytosolic region was highest after incubation at 2.8 mM glucose where it amounted 2.0±0.2 (n=19). This ratio was lowered by increasing glucose concentration and after incubation in 16.7 mM glucose it was significantly reduced to 1.3±0.1 (n=23; $p<0.01$). Syntaxin 1A fluorescence intensity (Fig. 1d) was slightly higher in the plasma membrane region than in the intracellular region only after incubation in 8.3 mM glucose; the glucose concentration at which glucagon secretion is most inhibited [33]. The ratio at this glucose concentration amounted to 1.1±0.1 (n=17) and was borderline significantly higher as compared to the ratio at 2.8 mM ($p=0.063$) and 16.7 mM ($p=0.052$) glucose, respectively.

As SNAP-25 and syntaxin 1A are both part of the SNARE-complex we next measured the co-localisation between SNAP-25 and syntaxin 1A at the different glucose-concentrations. As expected, we found that SNAP-25 co-localised with syntaxin 1A. The quantification revealed that 40±3% (n=22) of syntaxin 1A fluorescence was co-localised with SNAP-25 after incubation in 2.8 mM glucose which increased to 53±5% (n=18; $p=0.023$ vs 2.8 mM glucose) and to 70±4% (n=23; $p< 0.001$ vs. 2.8 mM and $p=0.031$ vs 8.3 mM) after incubation in 8.3 mM and 16.7 mM glucose, respectively.

Antibodies against SNAP-25 reduce exocytosis of glucagon-containing granules

The role of SNAP-25 in the exocytotic process of alpha-cells was investigated using capacitance measurements (Fig 2). In these experiments exocytosis was elicited by a train of ten 500 ms-depolarisations from -70 mV to 0 mV (Fig 2a-b). It has earlier been suggested that the capacitance increase evoked by the two first and latter eight depolarisations of a train represent the maximum size of the RRP and the refilling from RP, respectively [7]. We used this approach and applied an antibody against SNAP-25 intracellularly by inclusion in the pipette solution. The antibody against SNAP-25 clearly reduced the increase in membrane capacitance evoked by the train of depolarisations from 683±63 fF (n=12) under control condition to 274±68 fF (n=9; $p<0.001$). Closer inspection of the capacitance increase during the train of depolarisations revealed that the antibody against SNAP-25 has its main effect on mobilisation; inclusion of the antibody in the pipette solution led to a ~70% reduction in the capacitance increase during the latter eight depolarisations (Fig 2c) whereas the decrease during the first two depolarisations (i.e.

RPP) was ~45%. Thus, the data suggests that the antibody has the ability to interfere with both the RRP and refilling from the RP. The reduction in membrane capacitance in the presence of anti-SNAP-25 was not due to a decreased Ca^{2+}-current; the integrated Ca^{2+} current or charge (Q_{Ca}) during the first depolarization of the train was 8.8±1.4 pC (n=12) and 11.8±3.6 pC (n=9) in the absence and presence of the antibody, respectively.

It might be questioned whether antibodies block exocytosis simply by steric hindrance due to their bulky size. However, earlier data from our group have demonstrated that similar result is obtained when using the smaller Fab-fragments of an antibody as when using the full-size antibody [35]. In this study we performed control experiments using IgG to ascertain that the antibody did not reduce the exocytotic response simply by steric hindrance. When IgG was infused through the patch-pipette (Fig 2c), the increase in membrane capacitance evoked by the train amounted 681±145 fF (n=8, $p<0.01$ *vs* anti-SNAP-25; N.S *vs* control).

Alpha-cell exocytosis is reduced in the presence of antibodies against syntaxin 1A

Next, a train of ten 500 ms-depolarisations was applied on single alpha-cells in the absence and presence of an antibody against syntaxin 1A (Fig 3). In this series of experiments the capacitance increase evoked by the train amounted to 1640±133 fF (n=19) under control conditions. In the presence of anti-syntaxin 1A the increase in membrane capacitance was reduced to 922±240 fF (n=10; $p<0.01$ *vs* control). Exocytosis evoked by the first two depolarisations was reduced by ~50% ($p<0.01$) and the exocytotic response in the latter part of the train was reduced by ~30% ($p<0.05$) (Fig 3c). Hence, fusion of both primed and mobilised granules was significantly repressed by inclusion of anti-syntaxin 1A.

We have previously performed similar experiments in pancreatic beta-cells. In these experiments inclusion of the antibody against syntaxin 1A was associated not only by a reduced exocytotic response but also with a reduced Ca^{2+}-current [36]. The reduced Ca^{2+}-current could almost totally explain the reduced exocytotic response. We therefore examined if this is also true in pancreatic alpha-cells by measuring the Ca^{2+}-current in the absence and presence of the syntaxin 1A antibody (Suppl. Fig. 1). Voltage-dependent currents were elicited by 50 ms-depolarisations from -70 mV to voltages between -40 mV and +40 mV to investigate the current-voltage relationship (IV). These depolarisations stimulate the opening of both voltage-dependent Na^{+}-channels and Ca^{2+}-channels in the mouse alpha-cells, using the above described solutions. The voltage-dependent current is characterised by a peak-current constituted mainly by a rapidly inactivating (< 2 ms) Na^{+} current followed by a sustained current of Ca^{2+} ions. By measuring the mean size of the sustained current during the latter part of the depolarisation (25-50 ms) we certified that we evaluated the effects on the Ca^{2+}-current rather than on the Na^{+}-current. The largest sustained current was measured when depolarizing the single alpha-cells to +10 mV and the current amounted -22±2 pA (n=15) and -22±6 pA (n=8), in the absence and presence of anti-syntaxin 1A, respectively. Thus, unlike the situation in the beta-cell, anti-syntaxin 1A did not have any influence on the Ca^{2+}-current in mouse alpha-cells.

To investigate the impact of syntaxin 1A on rapid exocytosis we applied a protocol where the alpha-cell was subject to depolarisations from -70 mV to 0 mV of increasing pulse duration from 5 ms to 850 ms (Figs. 4a). Measurable exocytosis was elicited by depolarisations as short as 10 ms. Inclusion of anti-syntaxin 1A did not alter the response at depolarisations ≤100 ms. A 150 ms-depolarisation though, elicited a capacitance increase of 233±31 fF (n=15) under control

condition, which was reduced to 122±34 fF (n=8; $p<0.05$ *vs* control) in the presence of anti-syntaxin 1A. We next assessed the relationship between Ca^{2+}-entry and exocytosis under control conditions or in the presence of the syntaxin 1A-antibody. We therefore measured the Ca^{2+} -influx during the pulse durations (Fig 4c). No difference between groups was found, which confirms the IV-experiments described above. The slope of the relationship between the increase in membrane capacitance (ΔC_m) against the integrated Ca^{2+}-current (or charge; Q_{Ca}) is an estimate of exocytotic capacity at a given Ca^{2+}-concentration, referred to as the Ca^{2+}-sensitivity of exocytosis. Traditionally, this is performed using the mean data from each pulse duration. However, such pooling of data does not account for natural cell heterogeneity but assumes identical cells responses. We therefore utilized the capacitance data from the individual experiments summarised in Figs. 4b-c and used a mixed-effects statistical model [27]. This enabled us to investigate the difference in Ca^{2+}-sensitivity while allowing for random variation due to biological differences between cells. Within each group we considered a fixed effect of Ca^{2+} on exocytosis, which quantifies the Ca^{2+}-sensitivity, and included a random effect to adjust the model for how the individual cell responses deviate from the group estimates. The results of the analysis for each cell, either in absence and presence of anti-syntaxin 1A, are presented in Suppl. Fig. 2. Under control conditions the Ca^{2+}-sensitivity was estimated to 18±2 fF/pC (n=159 depolarisations in15 cells) and in the presence of anti-syntaxin 1A (n=77 depolarisations in 8 cells) the Ca^{2+}-sensitivity was reduced significantly ($p<0.05$ vs. control) to 10±3 fF/pC. In summary, anti-syntaxin 1A does not reduce the Ca^{2+}-current, but merely changes the Ca^{2+}-sensitivity of exocytosis, suggesting that the reduced exocytotic response in presence of anti-syntaxin 1A is mainly attributed to a direct effect on the exocytotic machinery.

Increased glucose concentration is associated with increased number of docked granules

Finally, we examined docking of glucagon containing granules at different glucose concentrations using ultrastructural analysis of electron microscope images. Islets were incubated at 1 mM, 8.3 mM and 16.7 mM glucose for 60 minutes prior to fixation and embedding. Electron micrographs from cells incubated in the different glucose concentrations can be observed in Fig 5a-c. First we measured the size of the glucagon granules after incubation at different glucose concentrations. The glucose concentration did not change the size of the granules and the diameter was 275±6 nm (n=589), 262±7 (n=433) and 267±5 (n=584) at 1 mM, 8.3 mM and 16.7 mM glucose, respectively. This was in agreement with previous measurements of the granule diameter in mouse pancreatic alpha-cells [2,12]. The total number of granules was estimated by calculation of the volume density of granules (N_v) within a alpha-cell. Although we found a tendency of increasing volume density with increasing glucose concentration, this did not reach significance and we conclude that there is no significant difference in the total number of granules between the different glucose concentrations (Fig 5d). To estimate the number of docked granules, the surface density (N_s) of granules situated within 150 nm (centre of the granule) from the plasma membrane was calculated. The number of docked granules increased with increasing glucose concentration and was more than two-fold higher ($p<0.001$) after incubation at 16.7 mM glucose compared to 1 mM glucose (Fig 5e). This is in line with earlier published data demonstrating that the rate of mobilisation of glucagon granules is increased with increased glucose concentration [26].

Discussion

The SNARE-proteins syntaxin 1A and SNAP-25 play central roles in exocytosis of most neuronal and (neuro)-endocrine cells [11,39]. We have earlier demonstrated that this is true also for the insulin-secreting beta-cell within the pancreatic islets of Langerhans [36]. Here we have investigated the importance and regulation of SNAP-25 and syntaxin 1A in the neighbouring glucagon-secreting alpha-cell using confocal microscopy and capacitance measurements. We have further investigated the glucose dependence of the docking process in this celltype.

In our study investigating the glucose-dependent localisation of SNAP-25 and syntaxin 1A, the ratio between the syntaxin 1A fluorescence intensity in the plasma membrane region compared to the cytosolic fraction was slightly higher at 8.3 mM glucose than after incubation at 2.8 mM and 16.7 mM glucose (Fig 1c), indicating a bell-shaped relationship between the glucose-concentration and the localisation of syntaxin 1A. It has been shown that following exocytosis, syntaxin molecules can diffuse away from the site of exocytosis [3], plausible also allowing internalization to occur. Considering this, reduced exocytosis in alpha-cells at 8.3 mM glucose could lead to an accumulation of releasable granules near the plasma membrane, which would prevent diffusion and internalisation of syntaxin 1A.

At all glucose concentration investigated syntaxin 1A was present in the cytoplasm (Fig 1a). Earlier data have suggested that syntaxin 1A is normally localised to the ER and golgi region when retained intracellularly [32] from where it needs to be transported to its site of action. Munc-18 has been implicated in transport of syntaxin 1A [32] and demonstrated to be phosphorylated by PKC [10]. More detailed studies are indeed needed in the future to be able to fully answer the question regarding syntaxin 1A trafficking in the alpha-cells but we have earlier shown that PKC plays an important role in the regulation of the pancreatic alpha-cell exocytosis [7].

It is well established that SNAP-25 localise to the plasma membrane through palmiotylation, and it has been suggested that syntaxin 1 is needed for the transport of SNAP-25 [32]. We observe a decreased fluorescence ratio with increasing glucose concentration, suggesting a movement of SNAP-25 into the cytoplasm (Fig 1a and d). In pancreatic beta-cells, desorption of cholesterol from the plasma membrane leads to re-localisation of SNAP-25 from the plasma membrane to the cytosol [35] which reduces exocytosis and insulin secretion. With that in mind, we hypothesize that high glucose concentrations result in loss of SNAP-25 in the plasma membrane, which in turn contributes to decreased glucagon secretion.

In our capacitance measurements on single mouse alpha-cells we observed a reduction in the exocytotic response by anti-SNAP-25, when measured as the total increase during the 10 depolarisations (Fig. 2C). The Ca^{2+}-current was not changed by the antibody against SNAP-25, suggesting that SNAP-25 mainly constitutes a unit of the exocytotic machinery as it does not have a direct effect on the Ca^{2+}-channels. It is still possible that a close coupling between the SNARE-proteins and the L-type Ca^{2+}-channels through the L-loop can exist, in similarity to observations in the beta-cells [37]. From our experiments (Fig 2c), it was clear that anti-SNAP-25 reduced both the RRP (by ~45%) and refilling from the RP (~70%). Why the reduction by the SNAP-25 antibody is strongest during mobilisation remains to be answered, but it has earlier been shown that SNAP-25 is of importance for mobilisation of granules [18].

Immunoneutralization of syntaxin 1A reduce exocytosis of both the RRP granules and granules mobilised from RP almost to the same extent (Fig. 3C) culminating in the assumption that syntaxin 1A is a requirement for fusion of granules in the alpha-cell. Granules released during depolarisations ≤100 ms belong to a small pool of immediately releasable granules (IRP) in close association with the Ca^{2+}-channels [2]. In our hands, the IRP was not as affected by the antibody as was the RRP. It has been suggested that the SNARE-complex can exist in either a tight or a loose formation [39]. If one then conjectures that the antibody cannot interfere with the SNARE-complex once it is in a tight formation it can be hypothesized that granules within the IRP are associated to the plasma membrane through a SNARE-complex in a tight formation or at least in a conformation unreachable for the antibody.

It is recognized that voltage-dependent Ca^{2+}-channels play a crucial role in pancreatic alpha-cell exocytosis [28]. In pancreatic beta-cells, part of the reduced exocytotic response in presence of anti-syntaxin 1A could be explained by a reduced Ca^{2+} -current. In contrast to the beta-cell Ca^{2+}-current, the voltage-dependent Ca^{2+}-current in the alpha-cell was not reduced by the antibody. How can this be explained? Our measurements where performed in the presence of cAMP where exocytosis is mainly dependent on influx though L-type Ca^{2+}-channels [6,14]. The beta-cell Ca^{2+}-current reduced by the antibody was a non-L-type and most likely a R-type Ca^{2+}-current [36] and alpha-cells do not contain R-type Ca^{2+}-channels [19]. Thus, it is not surprising that the antibody did not interfere with the Ca^{2+}-influx in the alpha-cells.

In alpha-cells synaptotagmin VII have been suggested to be the major Ca^{2+}-sensor in Ca^{2+}-depedent exocytosis [15]. Interestingly, syntaxin 1A has been demonstrated to bind to the Ca^{2+}-sensing C2A domain of synaptotagmins, including synaptotagmin VII [21]. In agreement, we found that the antibody against the N-terminal of syntaxin 1A used here reduced the Ca^{2+}-sensitivity of exocytosis by ~40%. This result is in agreement with earlier suggestions that mutation in, or interference with, the SNARE-complex leads to changes in Ca^{2+}-sensitivity [31,34-36]. Changes in the Ca^{2+}-sensitivity might be tremendously devastating for a cell such as the alpha-cell, where the Ca^{2+}-currents are much smaller as compared to neuronal cells, and small changes in the sensitivity (or the Ca^{2+}-influx) will have drastic effects on exocytosis and release of glucagon.

The electron microscopy investigation demonstrates that the number of docked granules is highest at 16.7 mM glucose. It should be mentioned that docking is defined as granules in the close vicinity to the plasma membrane including both primed and non-primed granules. During priming syntaxin 1A and SNAP-25 form a SNARE-complex together with VAMP2 on the docked granules to enable exocytosis [9,11]. Syntaxin 1A and SNAP-25 are plasma membrane bound proteins and so their decreased fluorescence at the plasma membrane at high glucose does not necessarily mirror the increased docking, but rather possibly the reduction in exocytosis.

To set the results from the ultrastructural analysis in perspective to the capacitance measurements one can estimate the number of total and docked granules within an alpha-cell. The volume density (N_v) at 1 mM glucose was estimated to 7 granules/μm^3 (Fig. 5d) and the surface density (N_s) to 0.4 granules/ μm^2 (Fig 5e). The volume and the surface area of an alpha-cell can be estimated to 624 μm^3 352 μm^2, respectively [2]. Hence, an alpha-cell contains ~4400 granules of which ~140 are docked at 1 mM glucose. That the pool of docked granules are not emptied during maximal stimulation at 1 mM glucose indicate that part of the docked pool consist of un-primed granules. The docked pool of granules increases to ~310 at 16.7 mM

glucose. Earlier published data have shown that secretion is reduced from ~40 pg/islet/h to ~20 pg/islet/h [32] when the glucose concentration is raised from 1 mM to 16.7 mM. These numbers correspond, respectively, to ~100 and ~50 granules/cell/h (based on a content of 2 ng glucagon/islet [17], 200-300 alpha-cells/islet and ~4400 granules/cell, giving an estimate of ~2fg glucagon/granule). Thus, out of the observed increase in the number of docked granules of ~170 per h only ~50 can be accounted for by reduced secretion. The remaining increase (~120 granules) is most likely due to increased docking. The reduced secretion might partly as discussed above be due to the reduced presence of SNAP-25 at the plasma membrane (Fig 1c) and the increased docking is most likely a result from increased mobilisation caused by the increased concentration of ATP at higher glucose concentration [25]. In summary, the increased number of docked granules at 16.7 mM glucose is a combination of reduced secretion and increased docking, where the majority (70%) is a result of the increased docking.

In conclusion, we identified for the first time how the temporal aspects of exocytosis is dependent on the SNARE-proteins syntaxin 1A and SNAP-25 in mouse pancreatic alpha-cells. We also showed that neither the antibody against syntaxin 1A nor anti-SNAP-25 reduced the voltage-dependent Ca^{2+}-current, suggesting that these SNARE-proteins regulate fusion as part of the exocytotic machinery, rather than through modulation of the Ca^{2+}-channel influx. Moreover, we estimate the number of granules in the alpha-cell to be ~4000 and demonstrate that granule docking in the alpha-cell is glucose-dependent.

Acknowledgements

We thank Britt-Marie Nilsson, Anna-Maria V Ramsay and Kristina Borglid for technical assistance. This work was supported by the Swedish Research Council, The Novo Nordisk foundation, The Swedish Diabetes Association, Knut and Alice Wallenberg Foundation, The Albert Påhlsson foundation and UMAS Foundation and the EU through a Marie Curie Intra-European Fellowship (MGP). LE is a senior researcher at the Swedish Research Council.

References

1. Barg S, Eliasson L, Renstrom E, Rorsman P (2002) A subset of 50 secretory granules in close contact with L-type Ca2+ channels accounts for first-phase insulin secretion in mouse beta-cells. Diabetes 51 Suppl 1:S74-82
2. Barg S, Galvanovskis J, Gopel SO, Rorsman P, Eliasson L (2000) Tight coupling between electrical activity and exocytosis in mouse glucagon-secreting alpha-cells. Diabetes 49 (9):1500-1510
3. Barg S, Knowles MK, Chen X, Midorikawa M, Almers W (2011) Syntaxin clusters assemble reversibly at sites of secretory granules in live cells. Proc Natl Acad Sci U S A 107 (48):20804-20809
4. Barg S, Renstrom E, Berggren PO, Bertorello A, Bokvist K, Braun M, Eliasson L, Holmes WE, Kohler M, Rorsman P, Thevenod F (1999) The stimulatory action of tolbutamide on Ca2+-dependent exocytosis in pancreatic beta cells is mediated by a 65-kDa mdr-like P-glycoprotein. Proc Natl Acad Sci U S A 96 (10):5539-5544
5. Cryer PE (2004) Diverse causes of hypoglycemia-associated autonomic failure in diabetes. N Engl J Med 350 (22):2272-2279
6. De Marinis YZ, Salehi A, Ward CE, Zhang Q, Abdulkader F, Bengtsson M, Braha O, Braun M, Ramracheya R, Amisten S, Habib AM, Moritoh Y, Zhang E, Reimann F, Rosengren AH, Shibasaki T, Gribble F, Renstrom E, Seino S, Eliasson L, Rorsman P (2010) GLP-1 inhibits and adrenaline stimulates glucagon release by differential modulation of N- and L-type Ca2+ channel-dependent exocytosis. Cell Metab 11 (6):543-553
7. De Marinis YZ, Zhang E, Amisten S, Taneera J, Renstrom E, Rorsman P, Eliasson L (2010) Enhancement of glucagon secretion in mouse and human pancreatic alpha cells by protein kinase C (PKC) involves intracellular trafficking of PKCalpha and PKCdelta. Diabetologia 53 (4):717-729
8. Detimary P, Dejonghe S, Ling Z, Pipeleers D, Schuit F, Henquin JC (1998) The changes in adenine nucleotides measured in glucose-stimulated rodent islets occur in beta cells but not in alpha cells and are also observed in human islets. J Biol Chem 273 (51):33905-33908
9. Eliasson L, Abdulkader F, Braun M, Galvanovskis J, Hoppa MB, Rorsman P (2008) Novel aspects of the molecular mechanisms controlling insulin secretion. J Physiol 586 (14):3313-3324
10. Fujita Y, Sasaki T, Fukui K, Kotani H, Kimura T, Hata Y, Sudhof TC, Scheller RH, Takai Y (1996) Phosphorylation of Munc-18/n-Sec1/rbSec1 by protein kinase C: its implication in regulating the interaction of Munc-18/n-Sec1/rbSec1 with syntaxin. J Biol Chem 271 (13):7265-7268

11. Gerber SH, Sudhof TC (2002) Molecular determinants of regulated exocytosis. Diabetes 51 Suppl 1:S3-11
12. Gopel S, Zhang Q, Eliasson L, Ma XS, Galvanovskis J, Kanno T, Salehi A, Rorsman P (2004) Capacitance measurements of exocytosis in mouse pancreatic alpha-, beta- and delta-cells within intact islets of Langerhans. J Physiol 556 (Pt 3):711-726
13. Gopel SO, Kanno T, Barg S, Weng XG, Gromada J, Rorsman P (2000) Regulation of glucagon release in mouse -cells by KATP channels and inactivation of TTX-sensitive Na+ channels. J Physiol 528 (Pt 3):509-520
14. Gromada J, Bokvist K, Ding WG, Barg S, Buschard K, Renstrom E, Rorsman P (1997) Adrenaline stimulates glucagon secretion in pancreatic A-cells by increasing the Ca2+ current and the number of granules close to the L-type Ca2+ channels. J Gen Physiol 110 (3):217-228
15. Gustavsson N, Wei SH, Hoang DN, Lao Y, Zhang Q, Radda GK, Rorsman P, Sudhof TC, Han W (2009) Synaptotagmin-7 is a principal Ca2+ sensor for Ca2+ -induced glucagon exocytosis in pancreas. J Physiol 587 (Pt 6):1169-1178
16. Hou JC, Min L, Pessin JE (2009) Insulin granule biogenesis, trafficking and exocytosis. Vitam Horm 80:473-506
17. Ishihara H, Maechler P, Gjinovci A, Herrera PL, Wollheim CB (2003) Islet beta-cell secretion determines glucagon release from neighbouring alpha-cells. Nat Cell Biol 5 (4):330-335
18. Jeans AF, Oliver PL, Johnson R, Capogna M, Vikman J, Molnar Z, Babbs A, Partridge CJ, Salehi A, Bengtsson M, Eliasson L, Rorsman P, Davies KE (2007) A dominant mutation in Snap25 causes impaired vesicle trafficking, sensorimotor gating, and ataxia in the blind-drunk mouse. Proc Natl Acad Sci U S A 104 (7):2431-2436
19. Jing X, Li DQ, Olofsson CS, Salehi A, Surve VV, Caballero J, Ivarsson R, Lundquist I, Pereverzev A, Schneider T, Rorsman P, Renstrom E (2005) CaV2.3 calcium channels control second-phase insulin release. J Clin Invest 115 (1):146-154
20. Lam PP, Leung YM, Sheu L, Ellis J, Tsushima RG, Osborne LR, Gaisano HY (2005) Transgenic mouse overexpressing syntaxin-1A as a diabetes model. Diabetes 54 (9):2744-2754. doi:54/9/2744 [pii]
21. Li C, Ullrich B, Zhang JZ, Anderson RG, Brose N, Sudhof TC (1995) Ca(2+)-dependent and -independent activities of neural and non-neural synaptotagmins. Nature 375 (6532):594-599.
22. Macdonald PE, Marinis YZ, Ramracheya R, Salehi A, Ma X, Johnson PR, Cox R, Eliasson L, Rorsman P (2007) A KATP Channel-Dependent Pathway within alpha Cells Regulates Glucagon Release from Both Rodent and Human Islets of Langerhans. PLoS Biol 5 (6):e143
23. Neher E (1998) Vesicle pools and Ca2+ microdomains: new tools for understanding their roles in neurotransmitter release. Neuron 20 (3):389-399
24. Olofsson CS, Gopel SO, Barg S, Galvanovskis J, Ma X, Salehi A, Rorsman P, Eliasson L (2002) Fast insulin secretion reflects exocytosis of docked granules in mouse pancreatic B-cells. Pflugers Arch 444 (1-2):43-51
25. Olsen HL, Hoy M, Zhang W, Bertorello AM, Bokvist K, Capito K, Efanov AM, Meister B, Thams P, Yang SN, Rorsman P, Berggren PO, Gromada J (2003) Phosphatidylinositol 4-kinase serves as a metabolic sensor and regulates priming of secretory granules in pancreatic beta cells. Proc Natl Acad Sci U S A 100 (9):5187-5192

26. Olsen HL, Theander S, Bokvist K, Buschard K, Wollheim CB, Gromada J (2005) Glucose stimulates glucagon release in single rat alpha-cells by mechanisms that mirror the stimulus-secretion coupling in beta-cells. Endocrinology 146 (11):4861-4870
27. Pinheiro JC, Bates DM (2009) Mixed-effects models in S and S-PLUS. Springer Verlag,
28. Quesada I, Tuduri E, Ripoll C, Nadal A (2008) Physiology of the pancreatic alpha-cell and glucagon secretion: role in glucose homeostasis and diabetes. J Endocrinol 199 (1):5-19
29. Rorsman P, Eliasson L, Renstrom E, Gromada J, Barg S, Gopel S (2000) The Cell Physiology of Biphasic Insulin Secretion. News Physiol Sci 15:72-77
30. Rorsman P, Salehi SA, Abdulkader F, Braun M, Macdonald PE (2008) K(ATP)-channels and glucose-regulated glucagon secretion. Trends Endocrinol Metab 19 (8):277-284
31. Sakaba T, Neher E (2003) Direct modulation of synaptic vesicle priming by GABA(B) receptor activation at a glutamatergic synapse. Nature 424 (6950):775-778
32. Salaun C, James DJ, Greaves J, Chamberlain LH (2004) Plasma membrane targeting of exocytic SNARE proteins. Biochim Biophys Acta 1693 (2):81-89
33. Salehi A, Vieira E, Gylfe E (2006) Paradoxical stimulation of glucagon secretion by high glucose concentrations. Diabetes 55 (8):2318-2323
34. Sorensen JB, Matti U, Wei SH, Nehring RB, Voets T, Ashery U, Binz T, Neher E, Rettig J (2002) The SNARE protein SNAP-25 is linked to fast calcium triggering of exocytosis. Proc Natl Acad Sci U S A 99 (3):1627-1632
35. Vikman J, Jimenez-Feltstrom J, Nyman P, Thelin J, Eliasson L (2009) Insulin secretion is highly sensitive to desorption of plasma membrane cholesterol. FASEB J 23 (1):58-67
36. Vikman J, Ma X, Hockerman GH, Rorsman P, Eliasson L (2006) Antibody inhibition of synaptosomal protein of 25 kDa (SNAP-25) and syntaxin 1 reduces rapid exocytosis in insulin-secreting cells. Journal of molecular endocrinology 36 (3):503-515
37. Wiser O, Trus M, Hernandez A, Renstrom E, Barg S, Rorsman P, Atlas D (1999) The voltage sensitive Lc-type Ca2+ channel is functionally coupled to the exocytotic machinery. Proc Natl Acad Sci U S A 96 (1):248-253
38. Xia F, Leung YM, Gaisano G, Gao X, Chen Y, Fox JE, Bhattacharjee A, Wheeler MB, Gaisano HY, Tsushima RG (2007) Targeting of voltage-gated K+ and Ca2+ channels and soluble N-ethylmaleimide-sensitive factor attachment protein receptor proteins to cholesterol-rich lipid rafts in pancreatic alpha-cells: effects on glucagon stimulus-secretion coupling. Endocrinology 148 (5):2157-2167
39. Xu T, Rammner B, Margittai M, Artalejo AR, Neher E, Jahn R (1999) Inhibition of SNARE complex assembly differentially affects kinetic components of exocytosis. Cell 99 (7):713-722
40. Yang SN, Larsson O, Branstrom R, Bertorello AM, Leibiger B, Leibiger IB, Moede T, Kohler M, Meister B, Berggren PO (1999) Syntaxin 1 interacts with the L(D) subtype of voltage-gated Ca(2+) channels in pancreatic beta cells. Proc Natl Acad Sci U S A 96 (18):10164-10169

Figures

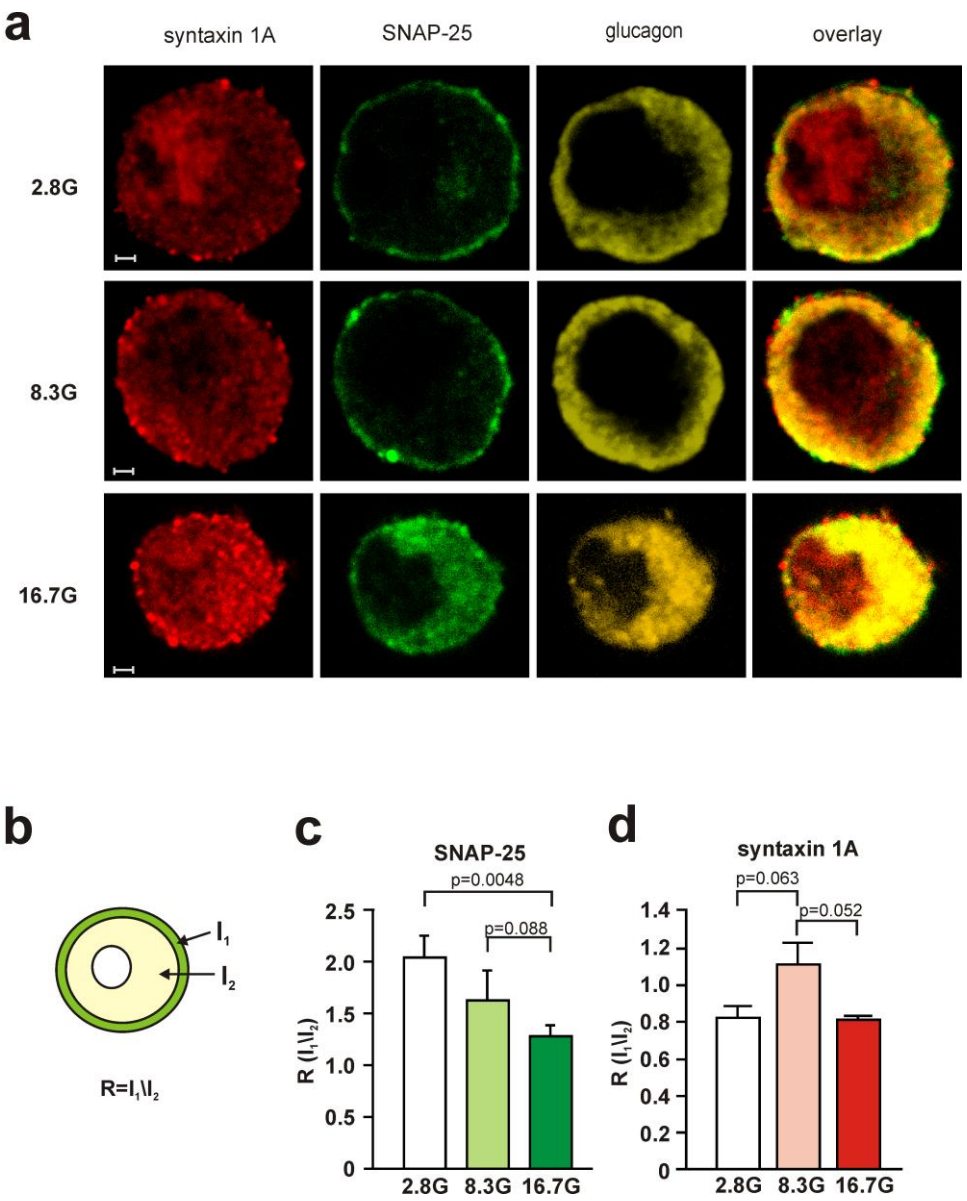

Fig. 1 Distribution of syntaxin 1A and SNAP-25 at different glucose concentrations in single mouse alpha-cells. a) Immunohistochemical labeling of syntaxin 1A (red), SNAP-25 (green), and glucagon (yellow) in single islet cells following 60 minutes of stimulation with 2.8, 8.3 and 16.7 mM glucose (G) as indicated. Notice the differential distribution of SNAP-25 and syntaxin 1A when varying the glucose concentration. Scale bar 2 µm b) Model illustrating the different areas in which fluorescence intensities have been measured. The fluorescence intensity I1 represent the plasma membrane and I2 the cytosolic region. The ratio R was calculated as described in *methods*. c) Histogram summarizing the ratio R at 2. 8, 8.3 and 16.7 G for the SNAP-25 fluorescence. d) Same as in c but for syntaxin 1A fluorescence. Data are mean values ± SEM of n=15-23 experiments. Significances were corrected using the Holm-Bonferroni method.

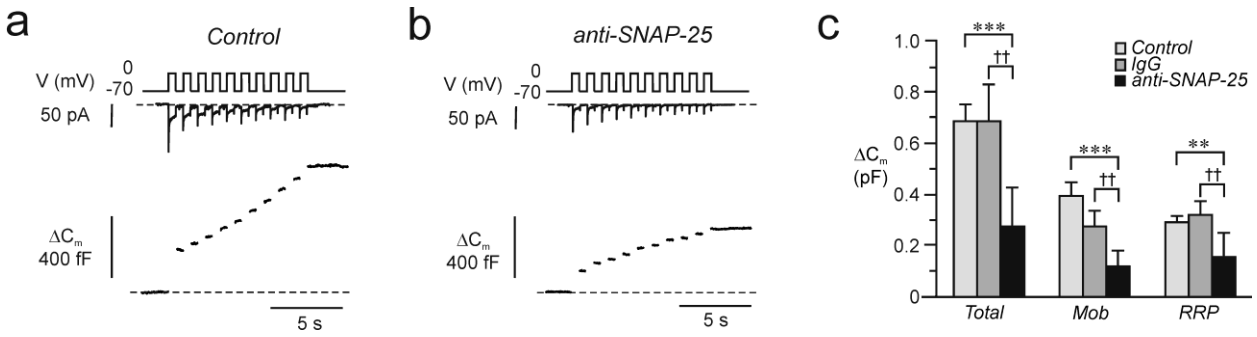

Fig. 2 The exocytotic response is decreased in presence of anti-SNAP-25 in mouse alpha-cells. a) Exocytosis, as measured by changes in membrane capacitance following a train of ten 500 ms depolarisations from -70 mV to 0 mV, in control setting in the absence of an antibody and using the standard whole-cell configuration b) As described in a, but after intracellular addition of anti-SNAP-25. c) Histogram of experiments in a and b summarizing the total increase in cell membrane capacitance (Total), mobilisation (Mob) and the Readily Releasable Pool (RRP) upon addition of anti-SNAP-25 (black bar) as compared to control (light grey bar) and addition of IgG (grey bar). Total represent the total increase in membrane capacitance evoked by the train. Mob is the capacitance increase as determined by pulses 3-10 in the train. The RRP is determined as the increase in membrane capacitance evoked by the first two depolarisations of the train. Data are mean values ± SEM of n=8-12 experiments. *** $p \leq 0.001$ and ** $p \leq 0.01$ anti-SNAP-25 *vs* control. ††$p < 0.01$ anti-SNAP-25 *vs* IgG.

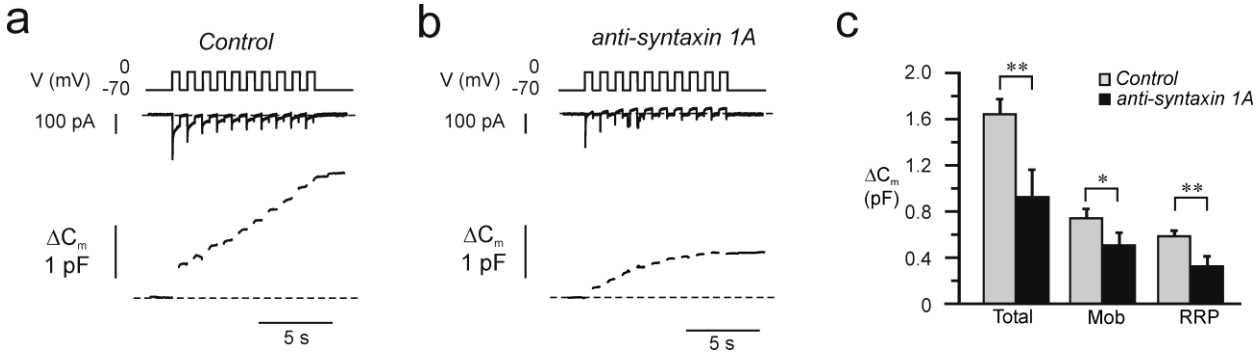

Fig. 3 Reduced alpha-cell exocytosis in presence of an antibody against syntaxin 1A. a) Exocytosis, as measured by changes in membrane capacitance following a train of ten 500 ms depolarisations from -70 mV to 0 mV, in control setting and using the standard whole-cell configuration. b) Same as in a, but upon intracellular addition of anti-syntaxin 1. c) Histogram of experiments in a and b summarizing the total increase in cell membrane capacitance (Total), mobilisation (Mob) and the Readily Releasable Pool (RRP) upon addition of anti-syntaxin 1A (black bar) as compared to control (grey bar). Total represent the total increase in membrane capacitance evoked by the train. Mob is the capacitance increase as determined by pulses 3-10 in the train. The RRP is determined as the increase in membrane capacitance evoked by the first two depolarisations of the train. Data are mean values ± SEM of n=10-19 experiments. * $p \leq 0.05$ and ** $p \leq 0.01$.

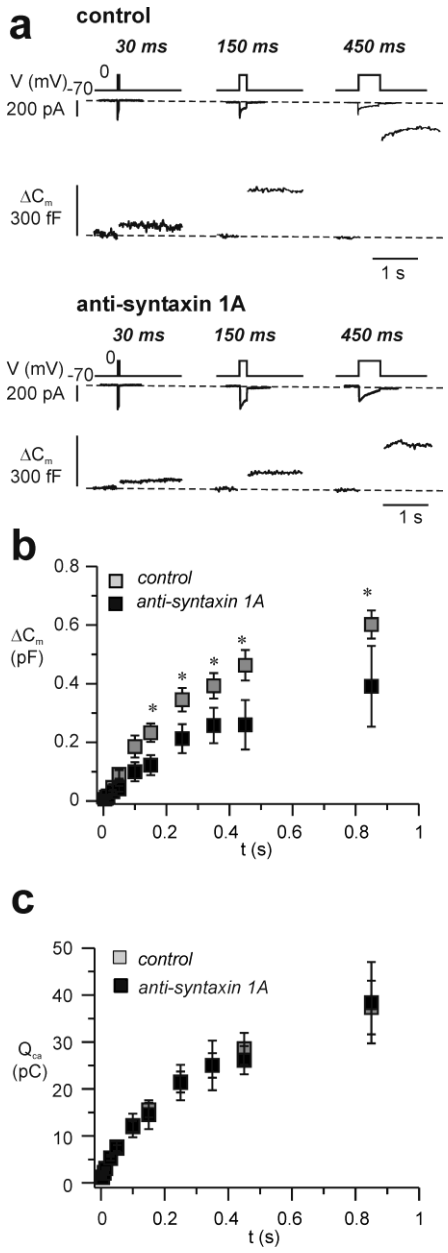

Fig. 4 Anti-syntaxin 1A reduce the RRP without reducing the Ca^{2+} current. a) Exocytosis, evoked by voltage-depolarisations (V) from -70 mV to 0 mV of increasing pulse duration ranging from 5 ms to 850 ms, was measured as increase in membrane capacitance (ΔC_m) under control conditions (*top*) and in the presence of anti-syntaxin 1A (*bottom*) in single mouse alpha-cells. Representative traces are presented for the 30-ms, 150-ms and 450-ms depolarization. b) Graph presenting data in a as the mean capacitance increase (ΔC_m) against the length of the depolarisation (t) under control conditions (grey) and in the presence of anti-syntaxin 1A (black). c) Summary of the Ca^{2+} entry (integrated Ca^{2+} current; Q_{Ca}) plotted against the length of depolarisation (t) under control conditions (grey) and in the presence of anti-syntaxin 1A (black). Data are mean values ± SEM of 8-15 experiments. * $p \leq 0.05$.

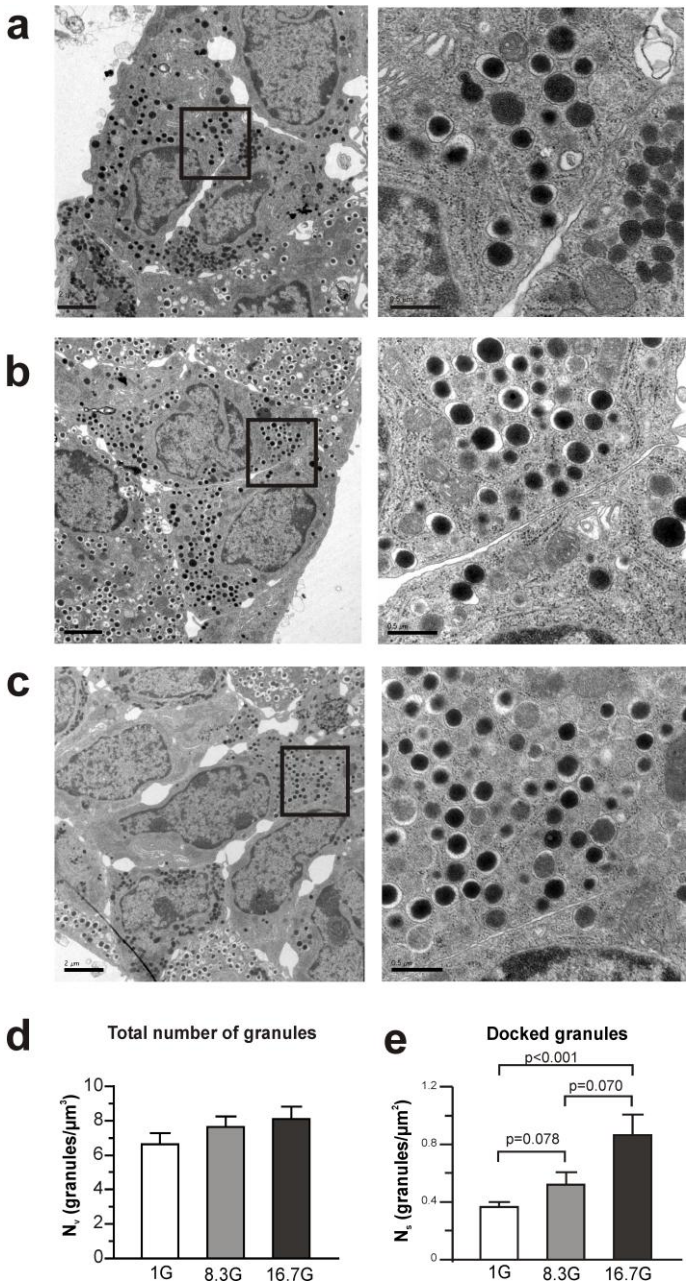

Fig. 5 Number of granules and number of docked granules at different glucose concentrations. a) Transmission electron micrograph of a single mouse alpha-cell within an islet (*left*; scale bar 2 µm) after incubation for 60 minutes in 1 mM glucose (G). The area within the square is highlighted to the *right* (scale bar 0.5 µm). b) As in a, but islets were incubated in 8.3 G prior to fixation. c) As in a, but islets were incubated in 16.7 G. d) Histogram summarising the total number of granules within single alpha-cells at 1, 8.3 and 16.7 G presented as the volume density (N_v). e) Histogram summarising the number of docked granules within single alpha-cells at 1, 8.3 and 16.7 G presented as the surface density (N_s). Calculations of N_v and N_s are described in "Methods" section. Data are mean values ± SEM of 18-24 experiments. Significances were corrected using the Holm-Bonferroni method.

Supplementary material

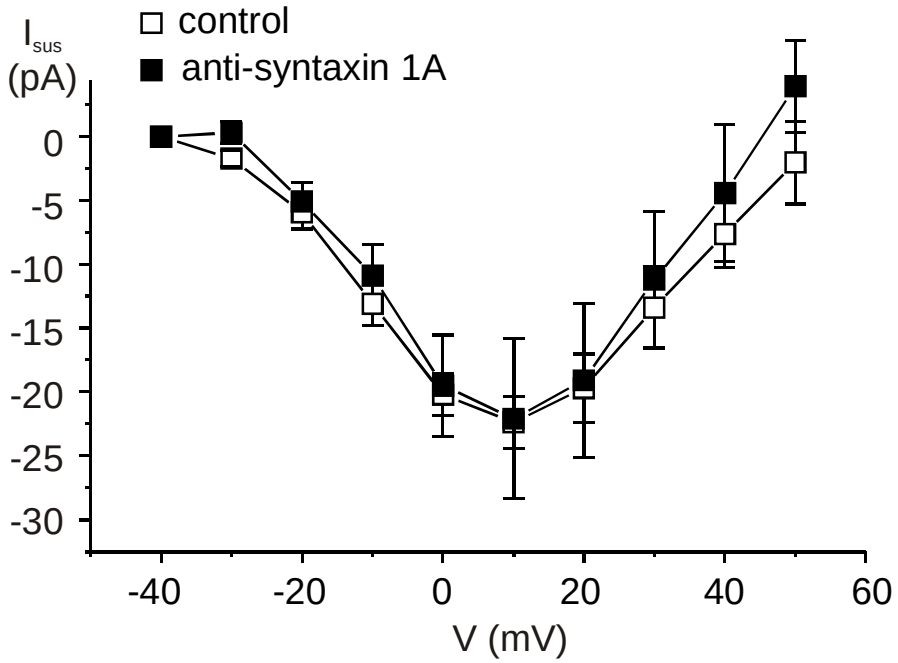

Suppl Fig. 1 Effects of anti-syntaxin 1A on the voltage-dependent Ca^{2+}-current. Current (I)-voltage (V) relationship of Ca^{2+}-currents recoded in the absence (white squares) and presence (black squares) of anti-syntaxin 1A. The currents were elicited by 50 ms-depolarisations from -70 mV to voltages between -40 mV and +40 mV. These depolarisations stimulate the opening of both voltage-dependent Na^{+}-channels and Ca^{2+}-channels. To be certain that effect on the Ca^{2+}-current were compared the mean current during the latter 25-50 ms was measured and plotted against the voltage. Data are presented as mean values ± SEM of 8-15 experiments.

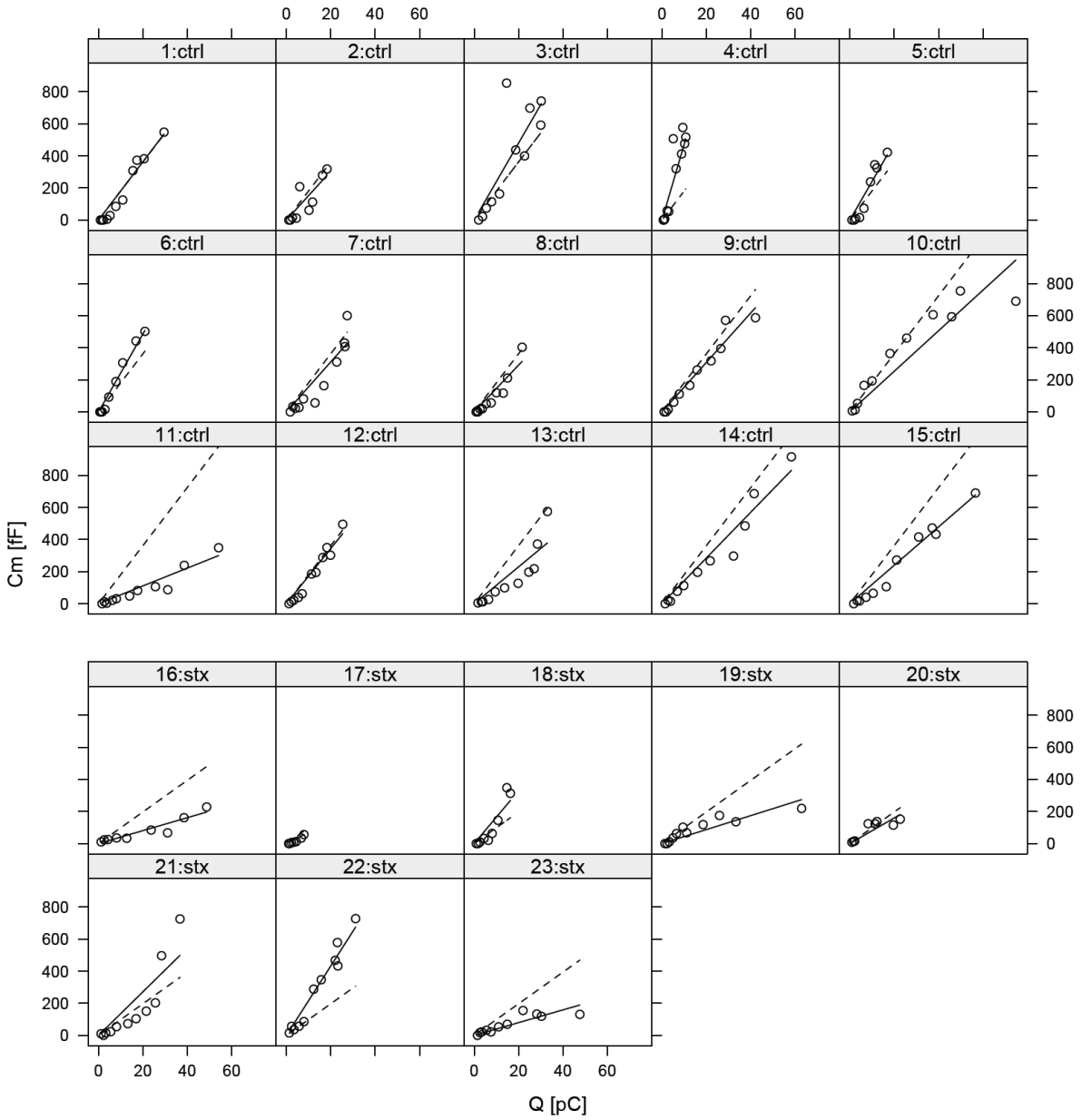

Suppl Fig. 2. Mixed-effects statistical model to estimate the Ca^{2+}-sensitivity of exocytosis. The graphs describe the results from individual experiments under control conditions (ctrl) or in the presence of anti-syntaxin 1A (stx) from the experiments presented in Fig. 4. Data for the individual experiments are presented as the increase in membrane capacitance (Cm) as a function of the Ca^{2+}-charge (Q). The fixed effect of Ca^{2+} on exocytosis, which quantifies the Ca^{2+}-sensitivity within each group, is indicated by the dotted line. The fits to data from individual experiments are indicated by the black, full curves. The random effect representing cell-to-cell variation accounts for the difference between cell (full) and group (dashed) fits.